Climatic influences on continental deposition during late-stage filling of an extensional basin, southeastern Arizona

GARY A. SMITH *Department of Earth and Planetary Sciences, University of New Mexico, Albuquerque, New Mexico 87131-1116*

ABSTRACT

Climatic, rather than tectonic, influences on continental deposition are recorded in the late-stage fill of a Neogene extensional basin in southeastern Arizona. Regional geomorphic relations, low sedimentation rates, and stratigraphic overlap of the principal basin-bounding structures identified in a gravity anomaly profile, indicate that the Plio-Pleistocene St. David Formation accumulated in the San Pedro Valley during a period of tectonic quiescence. Stable isotopic composition of paleosol calcite is placed within a magnetostratigraphic framework that provides an interpretive record of variable arid to semiarid climate in the valley. Before 3.4 Ma the valley was hydrologically closed and experienced an arid climate with seasonal precipitation. Drainage integration at ca. 3.4 Ma corresponds with a transition to wetter conditions, less seasonally variable precipitation, and a rising water table indicated by hydromorphic paleosols and pond deposits. Gradually increasing seasonality of precipitation after 2.8 Ma and further decrease in winter rainfall after 2.2 Ma led to establishment of a dry, monsoonal climate between 1.6 and 0.6 Ma. The change in climate at ca. 1.6 Ma coincides with abrupt appearance of sheet-flood–dominated fan gravels above earlier vertically aggraded fluvial-channel and interfluve–flood-plain deposits. This change in facies is interpreted as the result of climatic change rather than an example of subsidence-driven gravel progradation. Sedimentation rates were greatest when climate was relatively wet, with dominant winter rainfall, and about equally low for relatively dry, with dominant summer rain, and relatively wet, but nonseasonal, conditions. Contrary to past model simulations, channel:flood-plain–facies ratios and sedimentation rate varied directly. Ribbon, as opposed to sheet, channel bodies were favored by relatively wet climatic conditions and were less commonly formed during dry, strongly seasonal times. Precise process-response interpretation of this correlation of sedimentological variability to changing climate is limited by the restricted interpretation of paleosol-isotope paleoclimate data and the poor understanding of sedimentological response to climate change during 10^5- to 10^6-yr. time intervals. The results of this study suggest, however, that caution be applied to *a priori* interpretations of stratigraphic variations within thick syntectonic basin fills as responses to varying subsidence rates only.

INTRODUCTION

"Descriptions of sedimentary successions with inferences about tectonic control on sedimentation are legion, and this is hardly surprising in view of the fact that the major control on almost all sedimentation is tectonic" (Steel and others, 1977, p. 1124). Thus is stated one of the principal tenets of basin analysis that has guided most investigations of continental sedimentation for about two decades. Particular emphasis has been placed on the relationship of cyclic textural trends to postulated pulsating deformation along basin margins. Early studies related coarsening-upward cycles to episodic rejuvenation of relief in basin margin source areas and enhanced sediment production (for example, Steel and others, 1977; Wiltschko and Dorr, 1983; Mack and Rasmussen, 1984). More recently, fining-upward sequences have been attributed to periods of tectonic activity because of sourceward shifting of facies belts in asymmetric subsiding basins (for example, Blair and Bilodeau, 1988; Heller and others, 1988). Jordan and others (1988) have warned, however, that neither approach may be correct and that independent variables other than tectonism may account for the textural trends. Diffusion-based model simulations of gravel transport in subsiding basins offer insights into the origins of basin stratigraphic architecture (Paola and others, 1992; Heller and Paola, 1992) but remain general in nature.

Active tectonism is clearly of first-order importance to generate sources of, and depositories for, sediment in continental basins where subsidence is required for the accumulation of thick clastic successions. This paper, however, evaluates the extent to which climate accounts for stratigraphic variations within the basin fill.

Vertical textural trends in clastic basin fills can be explained as the result of climate change in semiarid or arid climatic zones where thresholds for sediment supply (both volume and grain size) are sensitive to changes in vegetation density and runoff-infiltration regimes. The best documented example of this effect is the widespread progradation of coarse-grained alluvial fans in response to early Holocene climate change (Bull and Schick, 1979; Mayer and others, 1984; Wells and others, 1987; Dohrenwend, 1987; Bull, 1991). Decrease in effective precipitation initiated time-transgressive changes in plant communities and diminished hill-slope vegetation densities that increased both sediment yield and runoff. The impact of this climate change was so profound that it controlled alluvial-fan sedimentation processes regardless of regional variations in tectonic activity (Bull, 1991). Although it might be argued that the frequency and extremes of climatic variation during the Quaternary are poor analogs for application to older sedimentary sequences, it is important to remember that the thresholds for climatic influences on alluvial sedimentation are not known.

The possible role of climatic fluctuations in generating stratigraphic variations that are currently interpreted, *a priori*, to result from episodic tectonism has not been adequately addressed. Where climatic influences are acknowledged, they have been inferred to be high-frequency effects related to Milankovitch orbital forcing and, therefore, distinguishable from longer-duration sedimentological changes attributed to tectonism (Blair and Bilodeau, 1988; Perlmutter and Matthews, 1990). This study attempted to avoid this ambiguity in control by investigating sedimentation during a long interval of tectonic quiescence at the end of basin subsidence and within the context of a local proxy climate record.

Geological Society of America Bulletin, v. 106, p. 1212–1228, 16 figs., September 1994.

GEOLOGIC SETTING

Location

The study area is the upper San Pedro Valley of southeastern Arizona (Fig. 1). The late Cenozoic stratigraphy and geomorphology of this valley have been the subject of classic studies of landscape evolution in a desert regime (for example, Bryan, 1926; Tuan, 1962; Melton, 1965). The principal exposed stratigraphic unit in the valley, and the subject of this paper, is the Pliocene–early Pleistocene St. David Formation (Fig. 2; Gray, 1965). Older basin-fill sediments are not exposed in the study area, and the composite exposed thickness of the St. David Formation is ~200 m. The St. David Formation is disconformably overlain by the middle(?) Pleistocene "granite wash" (Fig. 2; Gray, 1965), which underlies the highest basin-fill geomorphic surface (Bryan, 1926). A complex late Pleistocene and Holocene stratigraphy is represented by inset terrace units (Haynes, 1987). The northern boundary of the upper San Pedro Valley depositional basin is defined by a shallow bedrock bench at a point called "The Narrows," 20 km north of the town of Benson. No sedimentary units equivalent in age to the St. David Formation are known north of this feature (Dickinson, 1991).

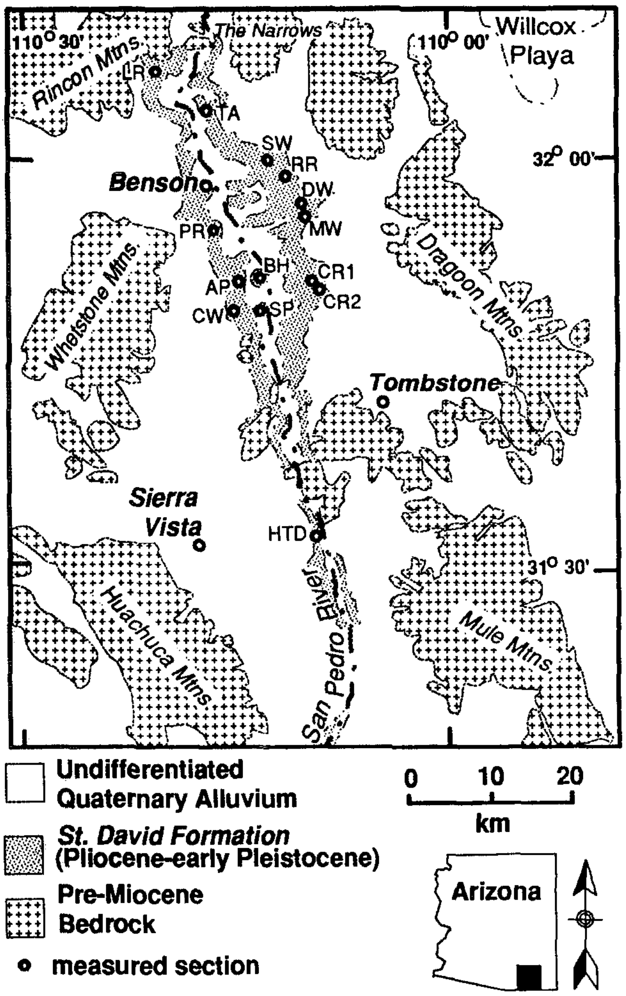

Figure 1. Map showing distribution of St. David Formation in the San Pedro Valley, Arizona. Measured sections, from north to south, are Little Rincon (LR); Tres Alamos (TA); Sheep Wash (SW); Railroad (RR); Dragoon Wash (DW); McRae Wash (MW); Post Ranch (PR); Apache Powder Plant (AP); Billy Hill (BH); Curtis Ranch (1 and 2) (CR); California Wash (CW); SP Hill (SP); and Horsethief Draw (HTD).

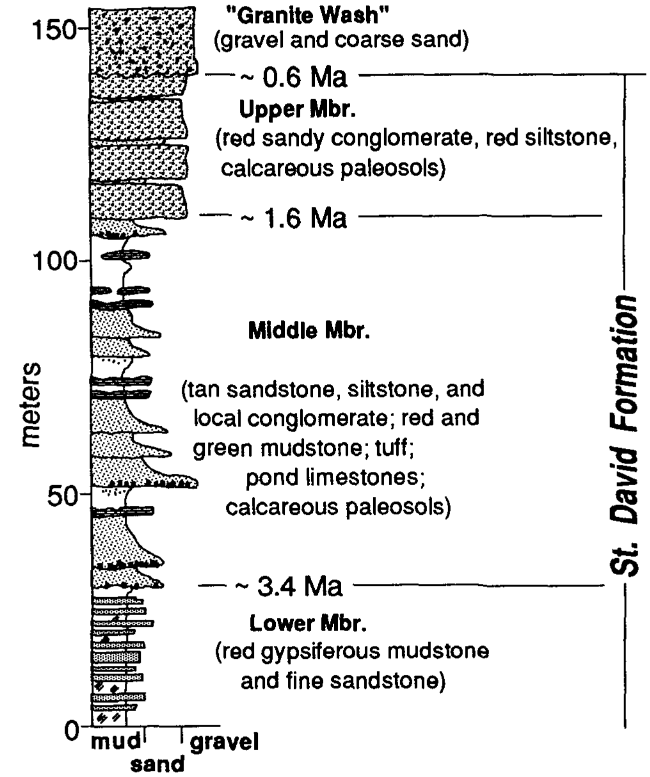

Figure 2. Generalized St. David Formation stratigraphy in the central San Pedro Valley, south of Benson, Arizona (after Gray, 1967; Lindsay and others, 1990a, 1990b).

Stratigraphy

Superb exposures of the St. David Formation in badlands along the San Pedro River and the lower piedmonts adjacent to the Dragoon, Whetstone, and Little Rincon Mountains (Fig. 1) have facilitated sedimentologic, magnetostratigraphic, and paleontologic studies. The St. David Formation has long been recognized as an important host for Blancan and Irvingtonian (Pliocene–early Pleistocene) vertebrate faunas (Lindsay, 1978, 1984). This biostratigraphic control was supplemented by important magnetostratigraphic studies (Johnson and others, 1975) that demonstrate an age of ca. 4.4–0.6 Ma for the exposed St. David Formation. Additional magnetostratigraphic data were collected during the present study (see below).

Gray (1965, 1967) established an informal stratigraphy of three members for the St. David Formation (Fig. 2). Later work (Lindsay and others, 1990a, 1990b) has shown that the lower and middle members exhibit greater lithologic diversity than was indicated by Gray, which makes their distinction difficult at some locations. Petrographic study by Gray (1965, 1967) and quantitative (Lindsay and others, 1990a) and qualitative examination of conglomerate and sandstone composition indicate no variation in sediment provenance during dep-

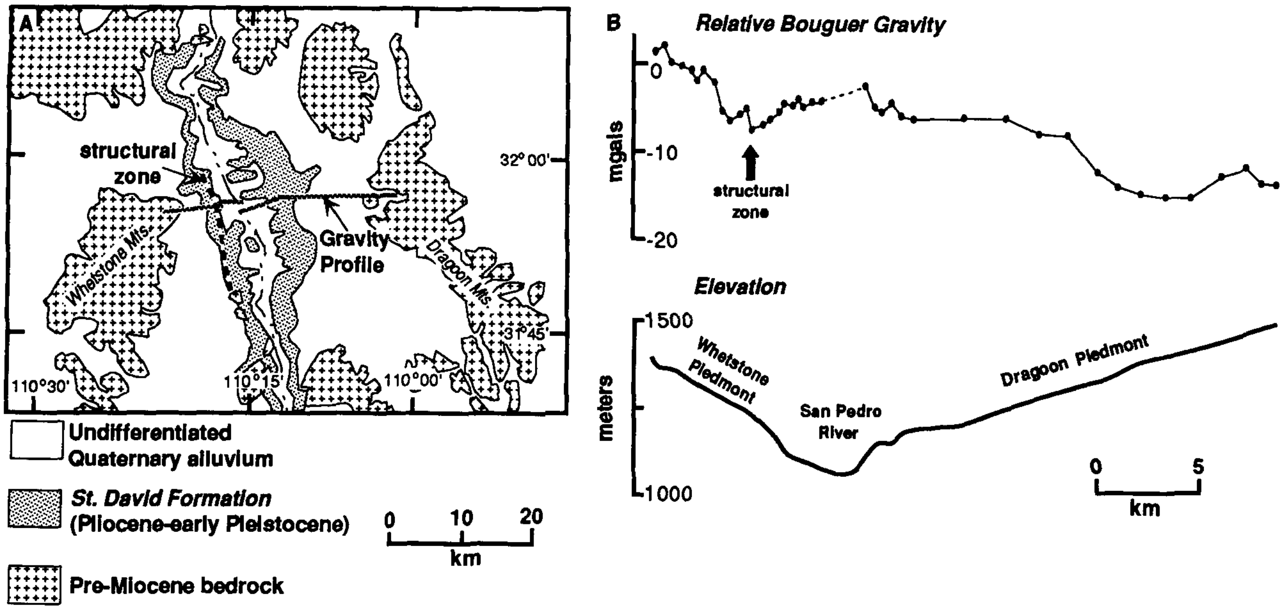

Figure 3. (A) Map showing trace of structural zone, expressed by faulted monocline in the St. David Formation, and line of gravity profile. (B) Relative Bouguer gravity anomaly and topographic profiles across the San Pedro Valley. Bouguer gravity values are plotted relative to the measured Bouguer gravity at the third station from the west (left) end of the profile. Stations at both ends of the profile rest on plutonic bedrock, suggesting that eastward decrease in Bouguer gravity is a regional gradient. The local gravity anomaly, therefore, is lowest under the Whetstone piedmont. The structural zone corresponds to a steep gradient in the profile. St. David Formation is undisturbed in the vicinity of other steep gradients to the west of the structural zone and near the San Pedro River.

osition of the St. David Formation. All three members and younger Quaternary sediments were derived from erosion of a diverse assemblage of Precambrian plutonic and metamorphic rocks, Paleozoic and Mesozoic sedimentary rocks, and Upper Cretaceous volcanic and plutonic rocks exposed in surrounding mountain ranges.

The lower St. David Formation consists primarily of red mudstone and fine sandstone with variable gypsum content. Only ~70 m of the lower member are exposed; water-well logs suggest at least 100 m of additional section in the subsurface.

The middle St. David Formation has traditionally been described as being dominated by red and green claystone, marl, distally erupted fallout tuff, and fine-grained tan sandstones (Gray, 1965; Johnson and others, 1975). In some areas of the basin, however, the middle St. David is composed almost entirely of medium- to coarse-grained sandstone and minor conglomerate (Smith and others, 1988; Lindsay and others, 1990a, 1990b). The boundary between lower and middle members appears to be contemporaneous throughout the basin; magnetostratigraphic data place this boundary close to the Gauss-Gilbert boundary, or at ca. 3.4 Ma (Johnson and others, 1975; Fig. 2).

The upper member of the St. David Formation rests abruptly, but with apparent conformity, upon the middle member. These uppermost St. David strata consist of red, poorly sorted, sandy granule-to-cobble conglomerate and pebbly sandstone that alternate with less abundant calcareous sandy siltstone.

St. David Formation deposition was terminated by basinwide incision in the early Brunhes Chron, at ca. 0.6 Ma (Fig. 2). Tens of meters of incision occurred before widespread deposition of the "granite wash" buried much of this erosional relief to establish the high basin-fill surface.

Tectonic Stability During Deposition

Basin and Range tectonic activity in southeastern Arizona greatly diminished in the late Miocene or earliest Pliocene (Melton, 1965; Menges and McFadden, 1981; Menges, 1983; Scarborough, 1984; Peirce, 1984; Morrison, 1985; Dickinson, 1991). This decline in tectonic activity is recorded by uppermost basin-fill strata that overlap range-front faults and rest on pediment surfaces cut on previously uplifted bedrock (Menges and McFadden, 1981; Peirce, 1984; Morrison, 1985). Concomitant with tectonic quiescence was an order of magnitude reduction in sediment accumulation rates (Menges and McFadden, 1981) and, consequently, a postulated increase in the importance of climate in controlling erosion and sedimentation (Menges and McFadden, 1981; Morrison, 1985).

A zone of minor structural deformation is expressed within the St. David Formation on the Whetstone piedmont as a narrow belt of high-angle normal faults and a monoclinal fold with a down-to-the-basin displacement of as much as 8 m (Fig. 3A). Scarborough and others (1983) interpreted this deformed zone as marking the buried structural margin of the Whetstone Mountains block; the deformation could then be envisioned as a minor reactivation of the overlapped range-front faults or differential compaction across them. These interpretations are consistent with the extent of Pliocene mountain-front retreat by pedimentation (as much as 7 km) that has been recognized elsewhere in southeastern Arizona (Menges and McFadden, 1981).

A Bouguer gravity profile across the valley (Fig. 3) reveals an anomaly of only ~10 mgal for the basin, consistent with a regional study based on widely spaced stations (Lysonski, 1981) and suggesting a lack of extremely thick, low-density sedimentary fill. The gravity profile further indicates structural asymmetry of the valley, also reflected by the topography, which is consistent with westward tilting of the valley floor. Two steps in the Bouguer profile indicate probable positions of basin-bounding faults under Whetstone piedmont deposits. One step coincides with the structural zone in the St. David Formation; the other is not expressed by deformation at the surface. The gravity data, therefore, corroborate the interpretation that St. David Formation deposition occurred during a period of nearly complete tectonic quiescence when mountain fronts were undergoing erosional retreat.

MAGNETOSTRATIGRAPHY

The magnetic properties of the St. David Formation were first described in the classic magnetic-polarity stratigraphy study of Johnson and others (1975). These earlier results were supplemented by the acquisition of additional polarity data from 91 sites, each site being a thin (<1.5 m) stratigraphic interval. All samples were subjected to alternating field demagnetization at field strengths from 2.5 mT to at least 100 mT. Selected samples were also thermally demagnetized over a temperature range of 60 to ~600 °C. Most samples exhibit a single component of magnetization, typically residing in a cubic magnetic phase, possibly magnetite. Consistency of demagnetization behavior and directional grouping at the site level indicate that these magnetizations are a detrital remanence acquired at, or locked in soon after, the time of deposition. The data permit correlation of the measured sections and establishment of the duration of deposition recorded at each section (Fig. 4). In coarse-grained facies, site spacing was not always close enough to record brief reversals, but the larger-interval reversal stratigraphy is consistent from section to section (Fig. 4).

CALCAREOUS PALEOSOLS AND PALEOCLIMATE

A proxy paleoclimate record for the San Pedro Valley was established by evaluating the carbon and oxygen isotopic compositions of pedogenic carbonate following the approach of Cerling and Hay (1986) and Cerling and others (1988, 1989). The C-isotopic composition is dependent on the nature of the flora that respire CO_2 in the soil (Cerling, 1984; Cerling and others, 1989). Trees, shrubs, and cool-season grasses, which use the C_3 photosynthetic pathway, produce a stronger depletion in ^{13}C than do C_4 plants, which mostly include warm-season grasses. Soil carbonate formed in the presence of only C_4 plants, generally under warm monsoonal conditions, has C-isotopic compositions near 0‰. Soil carbonate formed under wetter and generally less seasonal climates favoring dominance of C_3 plants is as depleted as −12‰. The carbon isotopic composition of unaltered soil carbonate, therefore, is a measure of the relative abundance of C_3 and C_4 plants, which are, in turn, indicative of ecological changes that are tied to seasonality of precipitation (Cerling, 1984; Cerling and Hay, 1986; Cerling and others, 1988, 1989). Empirical data demonstrate a close correlation between the oxygen isotopic composition of soil carbonate and meteoric water in the soil (Cerling, 1984; Quade and others, 1989). Temporal variations in oxygen isotopic composition, therefore, reflect variations in rainwater oxygen.

The isotope technique is applicable to samples from desert soil calcic horizons that formed in the unsaturated zone within sedimentary sequences. In modern soils, calcic horizons are present at the base of argillic-B horizons, usually >20 cm below the ground surface, from which calcite has been leached (Birkeland, 1984; Retallack, 1990). In nongravelly soils carbonate morphology progresses, with increasing development, from scattered filaments, to nodules, to massive layers (Gile and others, 1966; Machette, 1985). Carbonate content generally decreases downward within the calcic horizon. Increased carbonate-horizon maturity is accompanied by increased weathering, development of ped structure, and volume of translocated clay in the argillic horizon (Birkeland, 1984; Gile and others, 1966; Machette, 1985; Wright and Tucker, 1991).

Paleosols from which carbonate was sampled in the St. David Formation have several distinctive characteristics. The calcic horizons have sharp tops (Fig. 5A), exhibit a downward reduction in carbonate content, and are found below leached red mudstone with well-developed pedogenic fabrics that resemble argillic horizons (Slate and Smith, 1992; Smith and others, 1992; Wang and others, 1993). These calcic horizons are laterally continuous and generally have stage I or stage II morphology in the terminology of Gile and others (1966) and Machette (1985).

Carbonate was collected from St. David Formation paleosols throughout the basin, and the paleoclimatic interpretation presented below is summarized from the results of isotopic studies reported in Wang and others (1993) and Smith and others (1993). Carbon isotopic compositions of coexisting organic matter and calcite are consistent with the origin of the carbonate in soils without subsequent diagenetic alteration (Wang and other, 1993).

Lower member deposition occurred during a period of elevated carbon and oxygen values, suggesting relatively dry conditions with dominantly summer precipitation. The decrease in carbon isotopic compositions that commenced at ca. 3.4 Ma is consistent with a change to less seasonal conditions with greater effective precipitation. Sympathetic decrease in $\delta^{18}O$ is consistent with an increase in the ratio of winter to summer rainfall (Wang and others, 1993).

Through the remainder of middle member deposition, $\delta^{13}C$ values are markedly more variable than $\delta^{18}O$, apparently as a result of plant mosaicism (Wang and others, 1993). Plant mosaicism is also supported by the relatively low variation for carbonate samples collected from the same depositional settings (channel tracts, interfluve flood plains, and upper St. David alluvial fans), which are described in more detail in a later section (Fig. 6). Channel-tract and flood-basin floras were similar during the wettest, least seasonal period, 3.3–2.8 Ma. Increasingly seasonal precipitation after 2.8 Ma is indicated by increasing average $\delta^{13}C$ but different vegetational responses in adjacent depositional settings (Fig. 6). More C_3 plants (lower $\delta^{13}C$) in flood plains than near channels between 2.8 and 2.2 Ma imply sufficient moisture for C_3 plants in interfluves and frequent cool-season flooding that prohibited establishment of abundant trees or shrubs near channels. This generally moist but seasonal climatic interpretation is consistent with slightly diminished $\delta^{18}O$ values, which may indicate a continuing increase in the ratio of winter:summer rainfall. Limited $\delta^{13}C$ data suggest that by 2.0 Ma, there was insufficient year-round precipitation to sustain C_3 plants on interfluves, and riparian C_3 communities were developed in less frequently flooded channel-margin areas (Fig. 6). This interpretation of summer rain and winter drought is consistent with rising $\delta^{18}O$ values for flood-plain soils after ca. 2.2 Ma. Both $\delta^{13}C$ and $\delta^{18}O$ values are elevated and relatively stable during upper member deposition, indicating return to an arid monsoonal climate similar to the lower member time interval.

Not all carbonate accumulations in bioturbated mudstones in the St. David Formation exhibit the characteristics of the paleosols described above. Most of the thicker carbonate horizons (Fig. 5B) are

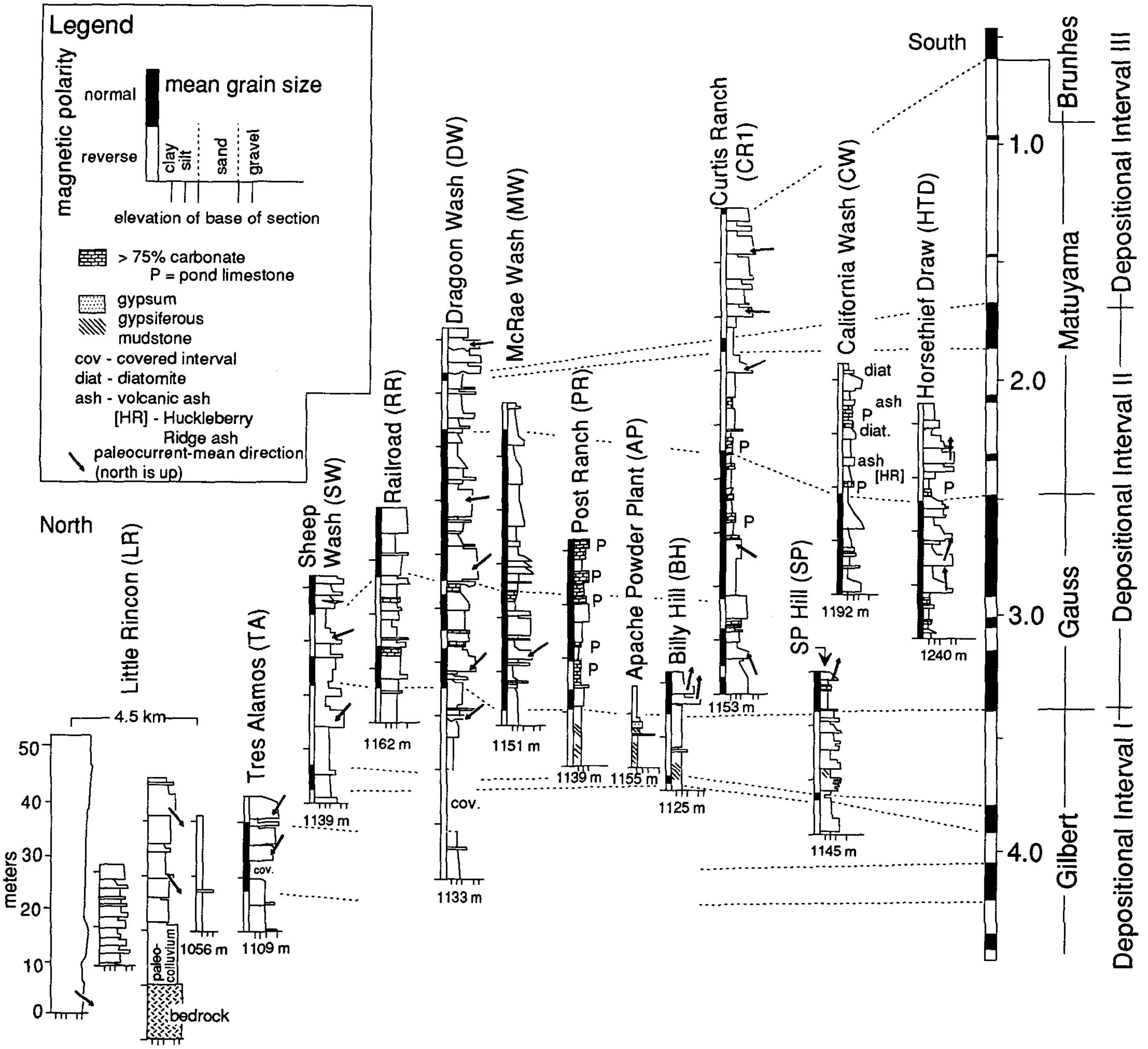

Figure 4. Magneto stratigraphy and generalized lithostratigraphy of the St. David Formation. Location of sections shown in Figure 1. CR sections are shown in greater detail in Figure 12. More detailed representations of BH, SP, and CW sections may be found in Lindsay and others (1990a). Most sections are composites of several closely spaced sections. All sections are overlain by granite wash. Most carbonate units that can be represented at this scale are pond limestone; others are hydromorphic-paleosol calcic horizons. Polarity-reversal stratigraphy for MW, PR, CR1, CW, and HTD sections is from Johnson and others (1975) and from Lindsay and others (1990a) for sections BH and SP. Remaining sections were the subject of magnetostratigraphic investigations as a part of this study. Correlation to the polarity reversal time scale of Harland and others (1990) is based on mammalian chronology and fission-track dates on volcanic ashes discussed by Johnson and others (1975). Dominance of coarse-grained facies in section LR precluded collection of meaningful magnetostratigraphic data; its position is approximated on the basis of elevation. Consistent polarity results were not obtained from section AP, possibly because of sediment displacement caused by dissolution and precipitation of gypsum; its position is approximated on the basis of proximity to section SP.

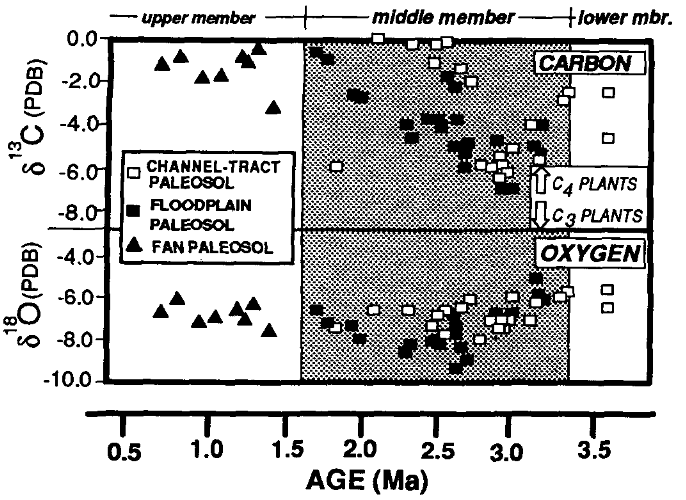

Figure 6. Carbon and oxygen isotopic values for 53 vadose-paleosol carbonate samples collected from St. David Formation along the east side of the San Pedro Valley (after Smith and others, 1993). Sample ages are interpolated from magnetostratigraphic data. Isotope data are plotted according to depositional environment because carbon values, in particular, differ in contemporaneous paleosols formed in different settings as a result of spatial variations in plant communities.

DEPOSITIONAL SUMMARY

The sedimentology of the St. David Formation was examined in detail at 14 measured sections (Figs. 1 and 4) and also in reconnaissance at more than 75 good exposures. These observations permit the construction of paleogeographic maps for three distinct depositional intervals. The transitions between these depositional intervals are, in most places, abrupt and nearly synchronous with polarity reversals, which facilitate their correlation throughout the basin.

Depositional Interval I: 4.4–3.4 Ma

The first depositional interval corresponds to the lower member of Gray (1965, 1967), where the members are distinctly defined in the central part of the basin. The top of this interval corresponds closely to the Gilbert-Gauss polarity boundary (Fig. 4). Strata of this age are exposed in a broad arc from the center of the valley north-northwestward to the flanks of the Rincon Mountains (Fig. 7A). Because the depth of modern valley dissection increases northward, and the overlying granite-wash–mantled unconformity also slopes northward, only sediments deposited near the beginning of this depositional interval are found at the northern outcrop margin, and only the youngest strata and the transition to depositional interval II are farther south (Fig. 4). Nonetheless, tracing of facies in outcrops suggests little lateral migration of depositional environments during this time interval. Exposed sections of interval I strata used for the reconstruction range in thickness from 10 to 60 m. Most of the sediments deposited during this time were fine sands and muds and record five semiconcentric facies belts (Fig. 7A).

Facies Pattern. Conglomerate crops out in a small area at the northwest edge of the valley. Within a distance of only 4.5 km, massive boulder gravel passes into tabular pebbly sandstone and on to massive mudstone (for example, Fig. 4, section LR). The paucity of channel forms and the abrupt lateral grain-size changes imply alluvial-fan deposits grading basinward into sandflats and mudflats. All of these deposits rest on pre-Tertiary bedrock (Fig. 8) that locally projects upward into the St. David Formation as paleohills, in some cases draped with paleocolluvium. Other small alluvial fans undoubtedly formed adjacent to mountain ranges fringing all sides of the valley, but exposures abutting the mountains are restricted to the northern basin margin.

Peripheral to the conglomerate, and also extending south-southeast along the edge of the badlands on the east side of the valley, is a belt of tabular, thin- to medium-bedded, medium- to coarse-grained sandstone interbedded with siltstone (Fig. 9). Most beds are internally massive, in some cases contain plane-parallel laminae, and typically are normally graded. Upward-coarsening units 20–50 cm thick are prominent in many outcrops. Pebbly horizons are present within the sands. In the northern part of the basins, these pebbles include distinctive, relatively fresh and typically vesicular volcanic rocks. These rock types are not present in adjacent mountain ranges and must have been introduced by drainages from the north and northeast, which drained Tertiary volcanic highlands (Dickinson, 1991). Transport from these directions is consistent with paleoflow directions dictated by pebble imbrications (Fig. 7A). Siltstones are generally bioturbated and rooted. Recognizable paleosols that include calcite nodules are rare. In the northeastern part of the outcrop belt, these strata are 20 m thick. Channel forms are conspicuously absent from most of this interval and first appear ~4 m below the Gilbert-Gauss polarity reversal. The tabular form of most beds (Fig. 9) suggests unconfined flow over broad, low-relief sandflats, at the toes of alluvial fans in the northwest and probably at the base of broad bajadas in the eastern basin. Transition from this sandflat facies assemblage to channeled streamflow deposits in the northern part of the basin represents a gradation, which is more abrupt farther south, from lower member piedmont facies to piedmont facies of the middle member.

Basinward of the sandflat facies belt are extensive exposures of deep-red siltstone and claystone more typical of the lower member as described by Gray (1965, 1967), covering an area of 80 km^2. These mudstone beds become generally finer-grained toward the center of the valley and consist of two different facies assemblages.

The sandflat deposits grade laterally into the first mudstone facies as sandy beds diminish in abundance to scattered, tabular, graded beds separated by several meters of massive or very rarely laminated mudstone. Depositional sedimentary structures are rare in the mudstones, and root traces are uncommon and restricted to thin horizons. All mudstone is at least slightly calcareous, and no recognizable paleosol horizons are defined. At widely spaced intervals the monotonous mudstone is interrupted by channels with epsilon cross-stratification indicative of point-bar deposition in meandering channels. These channel deposits range in thickness from 0.5 to 2.5 m and are <2 m wide in some basinward sections. Near the sandflat deposits, these channels are filled by fine to medium sand with discontinuous basal pebble lags. In more basinward sites, the channels typically are filled by very fine and fine sand with mud chips composing as much as 50% of individual beds. This facies assemblage appears to define a mudflat environment peripheral to the sandflats. Most deposition probably occurred by shallow overland flow, although widely spaced sinuous channels and gullies were formed. The massive character of the mudstone, despite the paucity of pedogenic and bioturbation features, suggests that the sediment was homogenized by shrink-swell processes associated with alternating wetting and drying. Desiccation also is indicated by the mud-chip grains in the channel fills.

The more basinward mudstone facies is notable for the complete lack of any channel- or gully-fill sediments and the ubiquitous pres-

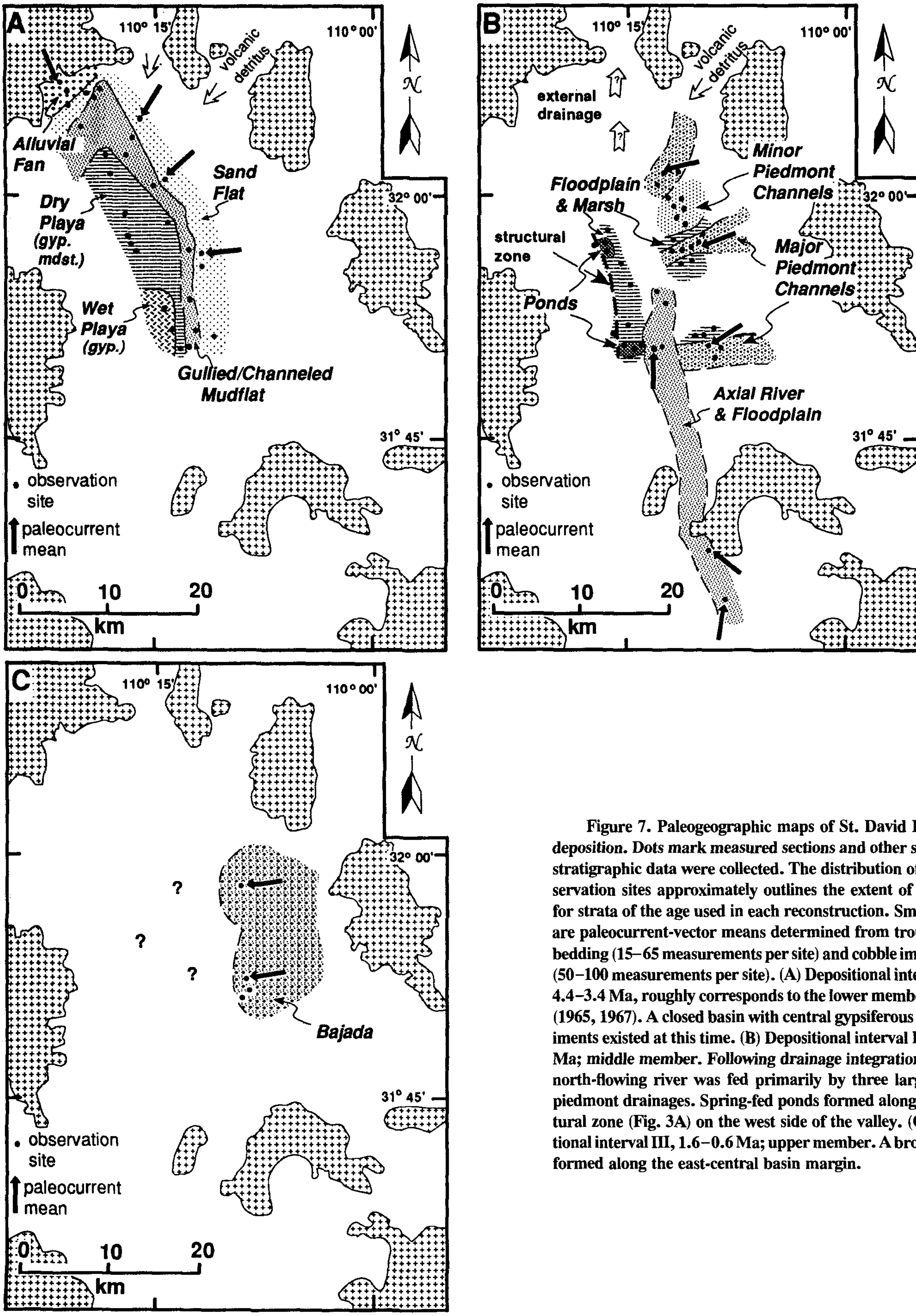

Figure 7. Paleogeographic maps of St. David Formation deposition. Dots mark measured sections and other sites where stratigraphic data were collected. The distribution of these observation sites approximately outlines the extent of exposures for strata of the age used in each reconstruction. Small arrows are paleocurrent-vector means determined from trough cross-bedding (15–65 measurements per site) and cobble imbrications (50–100 measurements per site). (A) Depositional interval I, ca. 4.4–3.4 Ma, roughly corresponds to the lower member of Gray (1965, 1967). A closed basin with central gypsiferous playa sediments existed at this time. (B) Depositional interval II, 3.4–1.6 Ma; middle member. Following drainage integration, an axial north-flowing river was fed primarily by three large eastern piedmont drainages. Spring-fed ponds formed along the structural zone (Fig. 3A) on the west side of the valley. (C) Depositional interval III, 1.6–0.6 Ma; upper member. A broad bajada formed along the east-central basin margin.

correspond roughly to the middle member of Gray (1965, 1967) and are extensively exposed in the central part of the valley (Fig. 7B). The thickest exposed sections (DW, MW, CR), as much as 70 m thick, are just east of the San Pedro River. Three general depositional settings are defined: axial fluvial, western piedmont, and eastern piedmont.

Facies Pattern. The axial fluvial deposits are marked by a narrow (<5 km) belt of ribbon-geometry conglomerate and trough–cross-bedded medium- to coarse-grained sandstone that is centered just west of the current San Pedro River channel (Fig. 4, sections BH, SP, HTD). Well-exposed channel bodies are 1.2–2.0 m thick and 15–30 m wide. Paleocurrent measurements indicate flow toward the north. In the central part of the valley, channel gravels are dominated by altered volcanic clasts (Lindsay and others, 1990a) identical to rock types exposed in Upper Cretaceous inliers in the southern part of the valley, near Tombstone (Fig. 1); the presence of these clasts also indicates northward transport. The ribbon channels are enclosed within mudstones and fine-grained sandstones representing deposition on an adjacent flood plain. Laminated green and red ostracodal mudstones and sparsely fossiliferous limestones represent ponds and marshes adjacent to main channels and in abandoned channels (Fig. 10). Thin (1–5 cm) graded strata form wedge-shaped levee deposits that become thinner and finer away from channels and grade into flood-plain and pond mudstone. Small (<1 m deep and 1–2 m across) channels filled with plane-parallel and ripple-laminated sandstone probably mark locations of crevasse channels. Hydromorphic paleosols with calcic horizons nearly 1.5 m thick prevail throughout the flood-plain deposits (Figs. 5B and 10).

The western piedmont deposits are dominated by mudstones and rare fine- to medium-grained sandstone that overlie the playa mudstone and gypsum of depositional interval I. Middle member mudstone lacks gypsum, has well-developed bioturbation and pedogenic fabrics, and contains both vadose- and hydromorphic-soil calcic horizons. The Post Ranch and California Wash areas (Fig. 1) are notable for laminated mudstone and limestone rich in charophyte and algal debris, ostracodes, and locally abundant gastropods and bivalves. The California Wash locality (Fig. 4, section CW) also contains diatomite (Lindsay and others, 1990a). The most extensive limestone near California Wash preserves the margins of a pond that covered ~6 km^2. Reworked ash-fall deposits are present in these pond and marsh deposits, including the ca. 2.0 Ma Huckleberry Ridge ash (Izett, 1981). The pond and marsh deposits at California Wash and Post Ranch can be traced upslope to abrupt depositional terminations within the structural zone along the lower Whetstone piedmont (Fig. 7B). This relationship suggests that the ponds and marshes were fed by springs rising along the buried fault trace.

Deposition on the eastern piedmont is represented by two very different facies recording channel tracts separated by swampy flood plains (Figs. 11 and 12). The three major channel tracts are ~3–5 km wide (Fig. 7B) and are characterized by stacked conglomerate and sandstone beds in generally upward-fining units 1.0–8.0 m thick, which are intercalated with thin (generally <1.5 m) sandy siltstone containing paleosols (Figs. 11A and 12). Most paleosols contain vadose calcic horizons, although all sections also contain hydromorphic calcic horizons in strata that are ca. 2.8–3.3 Ma. The hydromorphic paleosols are well developed only along the lower part of the piedmont and grade upslope to the east into typical vadose paleosols. Cross-bedding and cobble imbrications indicate westward flow. The northern channel tract contains Tertiary volcanic clasts like those in some lower member outcrops, implying a watershed that headed to the northeast of the valley. An area of smaller piedmont channels, in the vicinity of the Railroad (RR) section (Fig. 1), is mostly composed of bioturbated fine to medium sandstone and pebbly sandstone channel deposits <1.0 m thick. The three major channel tracts coincide roughly with the three largest arroyo systems on the modern piedmont, each of which heads in a large watershed along the eastern basin margin or northeast of the valley.

Although restricted to narrow tracts of the piedmont, these channels did migrate laterally short distances. In most outcrops, cross-bedded and plane-bedded channel sandstone and conglomerate grade laterally, across distances of 1–5 m, into massive, rooted and burrowed, pebbly sandstone. This transition was probably produced by bioturbation of channel sediments as the channel migrated laterally. The preservation of nonbioturbated channel-fill sequences up to 8 m thick and the absence of epsilon cross-stratification, however, suggest

Figure 10. Axial-river flood-plain deposits in section HTD (Fig. 1). Lenticular channel fine sandstone (S) is encased in massive mudstone with white, nodular hydromorphic-paleosol calcic horizons (H). Prominent ledge-forming carbonate layer (L) is a pond limestone overlying laminated mudstones (M); both facies contain ostracodes and gastropods.

Figure 11. Contrasting views of the channel-tract and flood-plain facies that were deposited on the eastern piedmont during depositional interval II. (A) Cross-bedded gravel and sand (above figure's head) resting on paleosol developed on another channel deposit; Dragoon Wash. (B) Flood-plain mudstone with intercalated calcareous ledges (marked by arrows) representing pond limestone and paleosol calcic horizons; Curtis Ranch.

that large-scale channel migration occurred by avulsion following periods of primarily vertical aggradation of channel and flood-plain deposits.

The channel tracts laterally merge abruptly with mudstone-dominated sections (Figs. 11B and 12) similar to those on the western piedmont, although they contain fewer marsh and pond deposits. The flood-plain tracts contain rare sharp-based, tabular plane-parallel and ripple-laminated fine sandstone that probably represents crevasse-splay sheets. Paleosols are developed throughout the flood-plain sections. Hydromorphic paleosols generally exist only in strata that are 2.8–3.3 Ma, although, in the Curtis Wash section (CW), hydromorphic soils, pond deposits, and spring tufas persisted to ca. 2.0 Ma.

Paleogeography. The transition from depositional interval I to interval II seems to record hydrologic opening of the valley (Fig. 7B). The bull's-eye facies pattern of interval I was replaced by an axial fluvial system fed by sizable piedmont drainage basins (Fig. 7). The presence of spring-fed ponds and marshes near the margin of the earlier playa and the prominence of hydromorphic paleosols suggest that interval II was marked by wetter conditions and elevated water tables, which is consistent with the paleosol–carbonate isotope records (Fig. 6). If the valley had remained enclosed, the resulting lake would have been restricted to the relatively small area in the northern part of the basin that lacks middle member exposures (Fig. 7B). This seems unlikely, however, because (1) this would have required a smaller lake than the playa that formed under the more arid conditions

Figure 12. Graphic representations of parts of sections CR1 and CR2 (see Fig. 1 for locations). Middle member facies undergo abrupt lateral transition from flood-plain (CR1) to channel-tract (CR2) deposits. Carbonate units thick enough to represent at this scale are pond limestones and hydromorphic-paleosol calcic horizons. The channel-tract and flood-plain facies are abruptly overlain by sheet-like, poorly sorted conglomerate of the upper member.

of interval I, and (2) this would have required an abrupt shift of the low area of the valley away from the base of the old footwall block to what had been topographically higher bajada sandflat and alluvial-fan settings during interval I.

The asymmetry of piedmont facies suggests that larger watersheds on the hanging-wall side of the basin provided more sediment and sustained larger streams than those on the footwall side. This relationship persists today, despite the lack of significant basin subsidence over the last 4–5 m.y. The tectonic legacy of the valley is recorded in this facies asymmetry and in the spring-fed ponds along the buried fault traces.

Depositional Interval III: 1.6–0.6 Ma

The upper member of the St. David Formation, deposited between ca. 1.6 Ma and the early Brunhes Chron (ca. 0.6 Ma), is exposed across a small area of the eastern piedmont in the central part of the valley (Fig. 7C). Because of the restricted preservation of the upper member, inferences about depositional characteristics and paleogeography are limited.

Facies Pattern. Eastern piedmont facies deposited during depositional interval III are tabular, poorly sorted, silty sandy conglomerate (Figs. 12 and 13). Unlike middle member channel bodies, upper member conglomerate is dominated by low-amplitude scour-and-fill structures and lacks regime-bedform deposits (for example, trough cross-beds). These attributes suggest that the flows were shallow and poorly confined. Interval III deposits lack pond facies or hydromorphic paleosols. The poorly sorted gravels form beds 2–6 m thick that are separated by sandy paleosols with calcic horizons (Figs. 5A and 13).

Paleogeography. The channels and flood plains that characterized the eastern piedmont during depositional interval II were abruptly replaced by a broad bajada of sheet-flood deposited sediment (Fig. 7C). Soils formed on these tabular sheet-flood deposits as depositional loci migrated on the margins of the large fans fed by ephemeral flow from the large watersheds of the hanging-wall block. This abrupt change in depositional style was coincident with the establishment of a dry, strongly monsoonal climate, based on the paleosol-carbonate isotope data (Fig. 6).

TEMPORAL VARIATIONS IN SEDIMENTATION PARAMETERS

Considerable attention has been given to the relationship of various sedimentological characteristics of basin fill to temporal varia-

Figure 13. Upper member exposures at Curtis Ranch. Tabular, poorly sorted, sandy-gravel sheet-flood deposits are separated by darker, finer-grained paleosols. Paleosol calcic horizon marked by arrow.

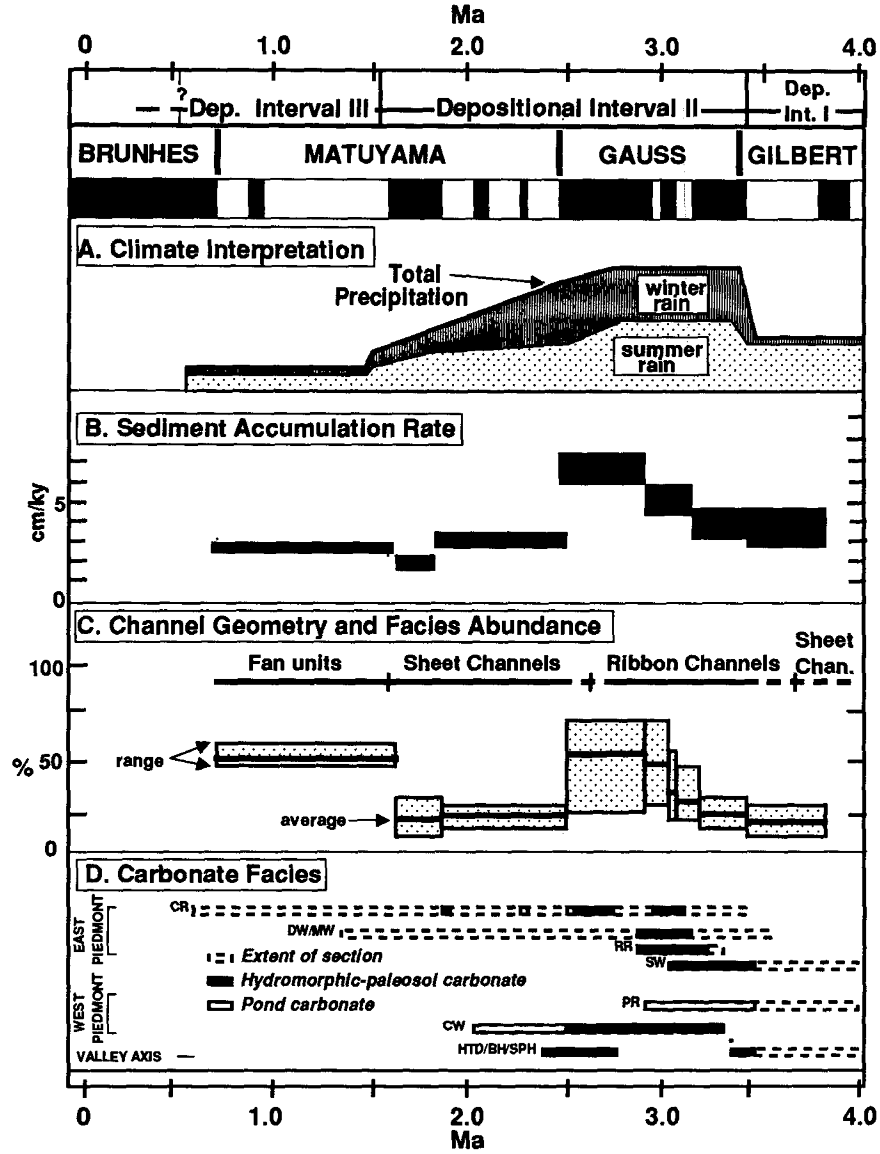

Figure 14. Summary diagram of paleoclimate interpretations and temporal variations in sedimentological characteristics within the chronologic control of the magnetic-polarity time scale of Harland and others (1990). See text for discussion. (A) Paleoclimatic interpretation of paleosol–carbonate isotope data (Fig. 6) as explained in text. (B) Sediment accumulation rates (not adjusted for compaction) averaged over time intervals defined by the magnetic polarity time scale. Bar widths reflect variations in rates determined from different stratigraphic sections and include uncertainties in the exact position of reversals in each section, which depends on spacing of paleomagnetic-sample sites. (C) Channel geometries (see also Fig. 16) and abundance of coarse channel facies in eastern piedmont sections. The average and range of the percentages of sections composed of sediment coarser than medium sand (Fig. 15) are shown over intervals defined by the polarity time scale to facilitate comparison to accumulation rates. Ranges for all sections and averages are shown; only channel-tract sections (SW, RR, DW, CR2) are represented for depositional interval II. (D) Temporal range of hydromorphic-paleosol and pond-carbonate rocks related to shallow water tables. Locations of sections shown in Figure 1.

tions in sedimentation and subsidence rates (for example, Bridge and Leeder, 1979; Kraus and Middleton, 1987; Paola, 1988; Paola and Heller, 1992; Heller and Paola, 1992). These studies focused on use of temporally varying sedimentological characteristics of terrestrial basins to elucidate their tectonic histories. Many of these sedimentological characteristics also can be examined in the St. David Formation (Figs. 14–16), where tectonic influences were probably minimal. The sedimentological changes in the St. David Formation coincide with inferred climatic changes that are recorded in the stable-isotopic compositions of the pedogenic carbonate horizons (Figs. 6 and 14). Interpretation of the variations in these characteristics as a response to climate changes is not altogether satisfying, however, because of the limitations of paleoclimate interpretations that can be ascertained from the paleosol-isotope data and the lack of understanding of fluvial responses to climate change. Although some of the conclusions presented below are admittedly conjectural, they are consistent with one another and form the basis for a hypothetical interpretation of sedimentological response to changing climate, rather than to variations in subsidence rates.

Sedimentation Rate

Within the magnetostratigraphic framework (Fig. 4), it is possible to examine temporal variations in net sediment accumulation rates averaged over time intervals defined by the polarity-reversal time scale. To alleviate the problem of partial dependence of sedimentation rates on the length of time interval over which the rate is calculated (Sadler, 1981; Sadler and Strauss, 1990), the rates are illustrated for time intervals of 0.2–1.1 m.y. (Fig. 14B). The accumulation rates, not adjusted for compaction, for the eastern piedmont sections range from ~2 to 7 cm/k.y. These rates are one to two orders of magnitude slower than undecompacted rates calculated for tectonically active basins during similar time intervals (Johnson, 1985; Jordan and others, 1988; Sadler and Strauss, 1990) and are consistent with the assertion that subsidence was not a significant control on deposition of the St. David Formation.

The threefold variation in sedimentation rate does, however, suggest an allogenic control. Because variable subsidence rates are unlikely to have had a significant effect, variations in sediment

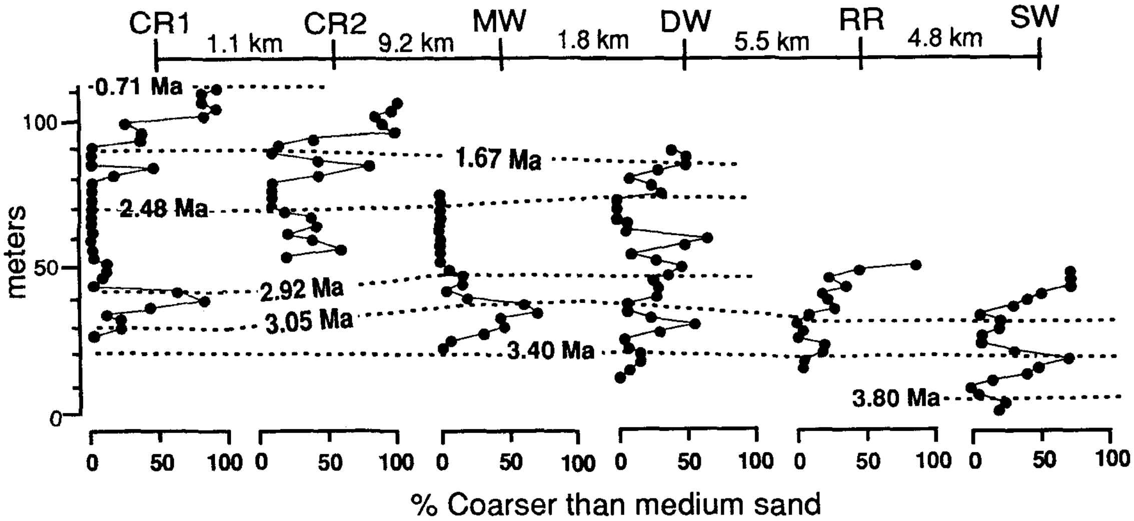

Figure 15. Five-meter running averages of the percentages of each eastern-piedmont section composed of facies coarser than medium sand, representing channel and proximal overbank facies. Lateral variability between closely spaced sections (CR1 and CR2, MW and DW) reflects the adjacent channel tracts and flood-plain interfluves that characterized the eastern piedmont during most of middle member deposition (Figs. 7B and 12). Time lines are derived from magnetostratigraphic data. Distances between sections shown; see Figure 1 for locations.

supply are implied. Relationships between climate, particularly rainfall, and sediment yield have been sought by many workers (Langbein and Schumm, 1958; Wilson, 1973; Yair and Enzel, 1987) with varied results that make generalizations impossible at this time (Graf, 1988). Nonetheless, Wilson's (1973) extensive database shows that sediment yield increases with total runoff and, hence, total precipitation, and that rates of fluvial erosion are greater for areas with strongly seasonal climate than for areas with nonseasonal climate. The variation in St. David Formation sedimentation rates may reflect such a climatic influence. The sedimentation rate increased during the period 3.2–2.4 Ma, which was a time of relatively high rainfall with increasing seasonality of precipitation based on interpretation of the paleosol-isotope data. Time intervals with dominant summer rainfall and generally low total rainfall, based on isotopic evidence for few C_3 plants, are characterized by lower sedimentation rates (Fig. 14).

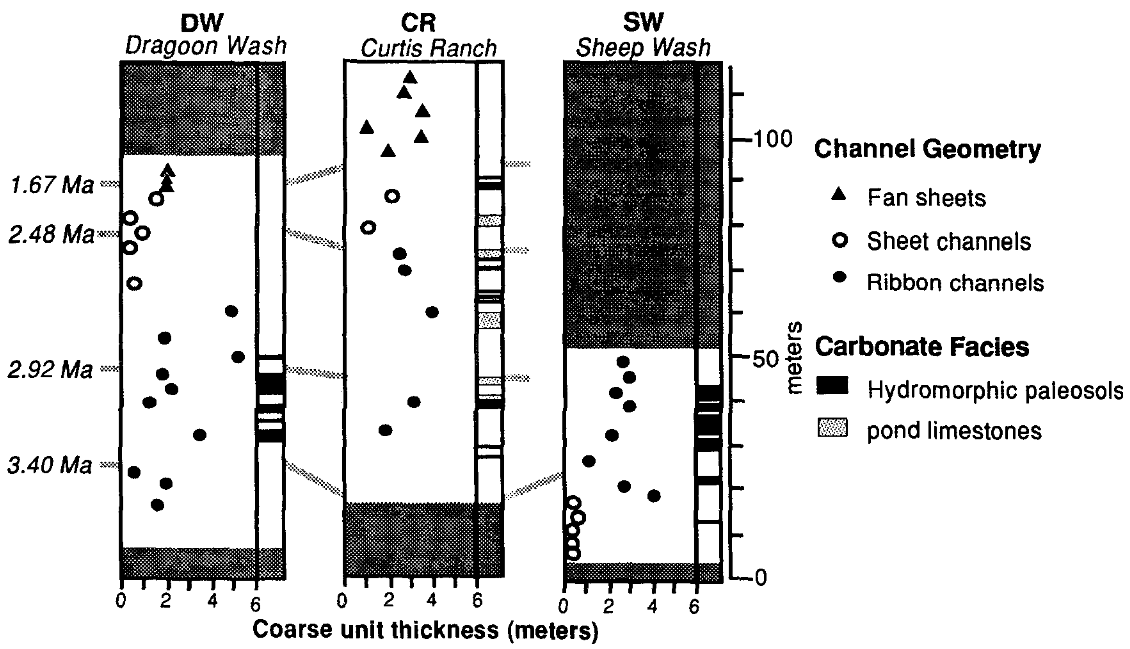

Figure 16. Stratigraphic variation in coarse-grained channel or fan-unit thickness and geometry, and carbonate facies indicative of high water tables for the three channel-dominated eastern piedmont sections (locations in Fig. 1). Thicknesses are total thickness of single-story units or thickness of thickest story in multistory units; upper St. David sheet-flood deposits are portrayed with the measured thickness between fine-grained paleosol layers (Fig. 13).

Channel:Flood-Plain Facies Ratios

Computer simulation models and field studies suggest that the ratio of preserved flood-plain sediments to channel facies deposited by meandering rivers should vary directly with subsidence rate, and hence with subsidence-induced sedimentation rate (Allen, 1978; Bridge and Leeder, 1979; Blakey and Gubitosa, 1984; Kraus and Middleton, 1987). Although there is no evidence for meandering streams on the St. David piedmonts, middle-member alluvium does suggest vertical accretion of channel fill followed by avulsion. Therefore, the concept of slower accumulation rates permitting more time for cannibalization of flood-plain sediments while channel deposits are retained is still generally applicable, and the ratio of coarse:fine facies should increase as the accumulation rate decreases (Allen, 1978; Jordan and others, 1988).

Coarse sediment abundance within eastern piedmont facies is generally higher between 3.2 and 2.5 Ma and after 1.67 Ma (Fig. 15). Although the temporal variation in grain size is great, when averaged over polarity-reversal time intervals, coarse sediment abundance is generally proportional to sedimentation rate (Fig. 14C). This relationship is the inverse of what is predicted by the fluvial simulation models of Allen (1978) and Bridge and Leeder (1979). Application of these models without the chronostratigraphic control provided by the magnetostratigraphy would potentially lead to conclusions about temporal variations in sedimentation rates that are the opposite of what is actually observed to be true.

The cause for sympathetic variation in sedimentation rate and coarse facies abundance is not clear. Possibly streams were more bedload-dominated during the relatively wet and seasonal conditions that prevailed when both sedimentation rates and coarse facies abundance were highest. Less competent mixed-load streams may have been favored under other climatic conditions leading to deposition of a greater thickness of flood-plain deposits. Whatever the reason, the data from the St. David Formation suggest that caution must be exercised in deducing relative sedimentation rates from coarse:fine facies ratios.

Channel Geometry and Depth

Paleohydraulic conditions may be qualitatively assessed by consideration of simple channel geometry and thickness (as a proxy for depth) of single-story channel bodies or the deepest channels within multistory bodies. These parameters were investigated in the three channel-tract sections (SW, DW, CR2) on the eastern piedmont (Fig. 16). Ribbon- and sheet-channel bodies were defined in the sense of Friend and others (1983). Ribbon channels were never seen to be interconnected within the extent of observable outcrop. Sheet bodies consist, in many cases, of laterally stacked channels indicative of a mobile channel belt (Friend and others, 1983), but the sand bodies themselves rarely appear to be interconnected, even where three-dimensional exposures are present over areas >1 km^2.

Sheet-form channel bodies were replaced by ribbon channels in the transition from depositional intervals I to II at ca. 3.4 Ma. Ribbon channels older than 3.4 Ma in the Dragoon Wash section are fine-grained bodies with prominent lateral-accretion surfaces typical of the channeled-mudflat facies belt of depositional interval I (lower member). Ribbon channels were replaced by sheet-channel bodies between 2.5 and 2.7 Ma. The thickest channel fills, representing the deepest channels, are in strata between ca. 3.2 and 2.8 Ma. The tendency for nonconnected ribbon channels to be in those parts of the section characterized by higher sedimentation rates is consistent with fluvial simulation models (Bridge and Leeder, 1979; Kraus and Middleton, 1987) despite the incongruity of a higher percentage of preserved flood-plain sediments associated with mobile–channel-belt sheet channels (Fig. 14).

The thickest channel fills were deposited during the time interval when the soil-isotope data suggest relatively wet, less seasonal climatic conditions (Figs. 6 and 14A). This period is also characterized by abundant hydromorphic paleosols in the piedmont deposits, suggesting a shallow water table (Figs. 14D and 16). Less variable discharges during this time may have favored development of relatively narrow, deep channels. Additionally, the isotope data indicate a prominence of C_3 trees and/or shrubs in near-channel areas during this time, which may have increased the stability of relatively narrow deep channels.

DISCUSSION

The St. David Formation probably accumulated after all significant basin-scale subsidence in the San Pedro Valley, although regional subsidence cannot be ruled out. The depositional overlap of geophysically identifiable basin-margin faults and very low aggradation rates support this conclusion. Post-tectonic sedimentation continued virtually uninterrupted until middle(?) Pleistocene and was followed by aggradation/degradation episodes recorded in post–St. David sediments (Lindsay and others, 1990a). Aggradation in the virtual absence of basin-scale subsidence suggests that duration of basin-fill sedimentation should not be equated with duration of active subsidence. The abrupt transition from internal to external drainage, defining the boundary between depositional intervals I and II, was not associated with significant base-level lowering and erosion, in contrast to the recent observations of a similar transition in the White River Valley, Nevada (DiGuiseppi and Bartley, 1991).

The transition from internal to external drainage at ca. 3.4 Ma is coincident with an abrupt decrease in $\delta^{13}C$ and $\delta^{18}O$ compositions of pedogenic carbonate (Fig. 6), which implies a change to less seasonably variable precipitation and probably wetter conditions. The water table also rose, presumably in response to this climate change, causing the development of a restricted area of wet playa deposits near the end of depositional interval I and the formation of hydromorphic soils and local spring-fed ponds early in depositional interval II (Fig. 14D). Although drainage integration could be a random phenomenon, the close correspondence of this process to sedimentological and geochemical indications of climate change suggest that increased runoff may have contributed to this event in the San Pedro Valley.

Between 3.4 and 2.5 Ma, the net sediment accumulation rate rose to its highest values, along with marked increases in the abundance of coarse-grained facies and the abundance of ribbon channels on the eastern piedmont (Figs. 14C and 16). Hydromorphic soils, denoting high water tables, formed locally on the eastern piedmont during this time and are prevalent in strata between 3.2 and 2.8 Ma. Isotopic values for vadose-paleosol carbonates suggest relatively cool and moist conditions with increasing seasonality of precipitation during this period, with a winter wet season. Hydromorphic soils formed mostly during the early period of least seasonal precipitation patterns. This was the wettest period of St. David deposition. Higher sedimentation rates may relate to increased runoff, especially when precipitation was more seasonal in distribution. Piedmont streams were bedload-dominated at this time, leaving a relatively small proportion of preserved flood-plain deposits despite the comparatively high sedimentation rates. Increased vegetation density may have contributed to channel stabilization and the development of relatively thick ribbon-channel bodies produced by avulsing channels that otherwise exhibited only limited lateral migration.

Between 2.5 and 1.7 Ma, the sedimentation rate diminished to its lowest value along with a sympathetic decrease in the abundance of coarse-grained units and a shift from ribbon to sheet channel geometry on the eastern piedmont (Fig. 14). Hydromorphic soil and pond carbonates virtually disappeared from the eastern piedmont but continued to form in the valley center, suggesting a descending water table (Fig. 14D). Isotopic compositions of soil carbonate suggest a warming trend and increasingly seasonal precipitation patterns consistent with a decrease in winter rainfall and an increase in summer rainfall. Increasingly flashy discharges and possible reduction of bank-stabilizing vegetation may have contributed to more mobile channel belts and the change from ribbon to sheet geometry for eastern piedmont channels. Decreased sedimentation rates may be a response to decreased runoff as aridity increased. Variable-competence flows were of more mixed-load character than before and deposited a greater proportion of flood-plain fines beyond shallow channel margins.

At ca. 1.6 Ma, the most abrupt change in eastern piedmont sedimentation style occurred with the transition from a channeled piedmont to a broad bajada (Fig. 8). Heller and Paola (1992) interpreted the transition from the relatively fine-grained middle member to coarser upper member as a coarsening-upward facies sequence that is consistent with their model progradation of coarse clastics as basin subsidence diminished. Several observations argue against this interpretation, however. First, field relationships limit the amount of basin-scale subsidence to <10 m during and after St. David Formation deposition, requiring an unlikely long lag time of >2 m.y. for the postulated subsidence-driven, modest-distance, gravel progradation following the cessation of significant basin subsidence. Second, the transition records an abrupt change in depositional morphology, not a gradual progradation of facies. Third, models of this type (Blair and Bilodeau, 1987; Heller and others, 1988; Paola and others, 1992; Heller and Paola, 1992) account for progradation of gravel from the structurally steepest side of an asymmetric basin. The asymmetry of modern topography, St. David Formation facies patterns, and the Bouguer gravity profile indicate westward tilting of the valley floor during extensional deformation, requiring the exposed upper St. David gravels to be shed from the hanging-wall block on the ramp side of the basin (that is, the opposite polarity from what is shown in Fig. 4 of Heller and Paola, 1992).

It seems unlikely that diminished subsidence can account for the sudden introduction of coarse-clastic detritus following several million years of relative tectonic quiescence when the mountain fronts underwent several kilometers of erosional retreat and already provided large volumes of sediment not accommodated by basin subsidence. Furthermore, enlargement of watersheds to provide large volumes of sediment for progradation during tectonic quiescence was already established by middle member time, based on the presence of the three prominent eastern piedmont channel tracts that coincide with the positions of the three largest piedmont channel systems present there today.

The transition from the middle member to the upper member coincides with the establishment of high, relatively invariant $\delta^{13}C$ and $\delta^{18}O$ values of pedogenic carbonate, signaling the complete establishment of a warm arid climate with a summer monsoon (Figs. 6 and 14A). Strongly episodic sedimentation by high-volume floods delivering sediment from sparsely vegetated hill slopes combined with diminished vegetative cover on the piedmont can account for the abrupt transition in facies in the manner modeled by Perlmutter and Matthews (1990) and interpreted for fan progradation accompanying Pleistocene-Holocene climate change in the southwestern United States (for example, Wells and others, 1987; Bull, 1991).

CONCLUSIONS

This study of the St. David Formation offers an evaluation of continental sedimentation in response to climate, rather than tectonics. Pliocene–early Pleistocene deposition in the San Pedro Valley occurred during nearly complete tectonic quiescence. The temporal variations in sedimentological characteristics of the St. David Formation are similar, however, to those that have been attributed to tectonic influences in studies of other fluvial sequences. Sedimentation rate, channel geometry, and facies abundance all vary sympathetically with the changing climatic conditions recorded in the pedogenic–carbonate isotope data. Precise process-response interpretation of the sedimentological changes in terms of climate forcing are not yet possible because of a lack of understanding of the effects of long-term climate change on fluvial and hill-slope geomorphic systems. Nonetheless, the lack of evidence for a significant tectonic influence and the covariance of climatic and sedimentologic parameters strongly suggest that climate can produce temporal variations in sedimentological processes that have heretofore been attributed only to tectonics. These variations in both climate and sedimentation were aperiodic during intervals of ~400–800 k.y. and do not, therefore, seem linked to high-frequency Milankovitch-scale climatic fluctuations.

Are these as yet poorly understood climatic influences on continental deposition also significant controls on stratigraphic architecture in rapidly subsiding basins? This question cannot be answered at this time. But the results of this study suggest (1) application of caution in asserting tectonics as the only significant long-time-period influence on depositional style in nonmarine basins, and (2) the need for better understanding of climatic effects on hill-slope processes and drainage basin evolution that regulate sediment supply and fluvial processes that deliver sediment to depositional sites, especially over time intervals of 10^5–10^6 yr.

ACKNOWLEDGMENTS

This research was supported by National Science Foundation Grant EAR 89-16355. I especially thank Danny Katzman for invaluable assistance in stratigraphic studies and sampling. J. W. Geissman and R. Livacarri performed paleomagnetic analyses; E. H. Lindsay provided detailed site locations from the Johnson and others (1975) magnetic-polarity study; Y. Wang and T. E. Cerling completed the parallel, and essential, isotopic studies for paleoclimatic interpretations. The 1989 University of New Mexico exploration geophysics class and John Geissman collected the gravity-profile data. The Bureau of Land Management San Pedro Riparian National Conservation Area provided field accommodations. The manuscript was improved by reviewers Greg Mack and Jim Schmitt and especially by *Bulletin* Associate Editor Peter DeCelles and Editor Art Sylvester.

REFERENCES CITED

Allen, J. R. L., 1978, Studies in fluviatile sedimentation: An exploratory quantitative model for the architecture of avulsion-controlled alluvial suites: Sedimentary Geology, v. 21, p. 129–147.
Birkeland, P. W., 1984, Soils and geomorphology: New York, Oxford University Press, 372 p.
Blair, T. C., and Bilodeau, W. L., 1988, Development of tectonic cyclothems in rift, pull-apart, and foreland basins: Geology, v. 16, p. 517–520.
Blakey, R. C., and Gubitosa, R., 1984, Controls of sandstone body geometry and architecture in the Chinle Formation (Upper Triassic), Colorado Plateau: Sedimentary Geology, v. 38, p. 51–86.
Bridge, J. S., and Leeder, M. R., 1979, A simulation model of alluvial stratigraphy: Sedimentology, v. 26, p. 617–644.
Bryan, K., 1926, The San Pedro Valley, Arizona, and the geographical cycle [abs.]: Geological Society of America Bulletin, v. 37, p. 169–170.
Bull, W. B., 1991, Geomorphic responses to climatic change: New York, Oxford University Press, 326 p.
Bull, W. B., and Schick, A. P., 1979, Impact of climatic changes on an arid watershed, Nahal Yael, southern Israel: Quaternary Research, v. 11, p. 153–170.
Cerling, T. E., 1984, The stable isotopic composition of modern soil carbonate and its relationship to climate: Earth and Planetary Science Letters, v. 71, p. 229–240.
Cerling, T. E., and Hay, R. L., 1986, An isotopic study of paleosol carbonates from Olduvai Gorge: Quaternary Research, v. 25, p. 63–78.
Cerling, T. E., Bowman, J. R., and O'Neil, J. R., 1988, An isotopic study of a fluvial-lacustrine sequence: The Plio-Pleistocene Koobi Fora sequence, East Africa: Palaeogeography, Palaeoclimatology, Palaeoecology, v. 63, p. 335–356.
Cerling, T. E., Quade, J., Wang, Y., and Bowman, J. R., 1989, Carbon isotopes in soils and paleosols as ecology and palaeoecology indicators: Nature, v. 341, p. 138–139.
Dickinson, W. R., 1991, Tectonic setting of faulted Tertiary strata associated with the Catalina core complex in southern Arizona: Geological Society of America Special Paper 264, 106 p.
DiGuiseppi, W. H., and Bartley, J. M., 1991, Stratigraphic effects of change from internal to external drainage in an extending basin, southeastern Nevada: Geological Society of America Bulletin, v. 103, p. 48–55.
Dohrenwend, J. C., 1987, Basin and Range, *in* Graf, W. L., ed., Geomorphic systems of North America: Geological Society of America Centennial Special Volume 2, p. 303–342.
Freytet, P., and Plaziat, J.-C., 1982, Continental carbonate sedimentation and pedogenesis—Late Cretaceous and early Tertiary of southern France: Stuttgart, Federal Republic of Germany, E. Schweiaerbart'sche Verlagsbuchhandlung, 262 p.
Friend, P. F., 1983, Towards a field classification of alluvial architecture or sequence, *in* Collinson, J. D., and Lewin, J., eds., Modern and ancient fluvial systems: International Association of Sedimentologists Special Publication 6, p. 345–354.
Gile, L. H., Peterson, F. F., and Grossman, R. B., 1966, Morphological and genetic sequences of carbonate accumulation in desert soils: Soil Science, v. 101, p. 347–360.
Graf, W. L., 1988, Fluvial processes in dryland rivers: Berlin, Federal Republic of Germany, Springer-Verlag, 346 p.
Gray, R. S., 1965, Late Cenozoic sediments in the San Pedro Valley near St. David, Arizona [Ph.D. thesis]: Tucson, University of Arizona, 198 p.
Gray, R. S., 1967, Petrography of the Upper Cenozoic non-marine sediments in the San Pedro Valley, Arizona: Journal of Sedimentary Petrology, v. 37, p. 774–789.
Harland, W. B., Armstrong, R. L., Cox, A. V., Craig, L. E., Smith, A. G., and Smith, D. G., 1990, A geologic time scale 1989: Cambridge, England, Cambridge University Press, 263 p.
Haynes, C. V., Jr., 1987, Curray Draw, Cochise County, Arizona: A late Quaternary stratigraphic record of Pleistocene extinction and paleo-Indian activities: Geological Society of America Centennial Field Guide, Cordilleran Section, p. 23–28.
Heller, P. L., and Paola, C., 1992, The large-scale dynamics of grain-size variation in alluvial basins, 2: Application to syntectonic conglomerate: Basin Research, v. 4, p. 91–102.
Heller, P. L., Angevine, C. L., Winslow, N. S., and Paola, C., 1988, Two-phase stratigraphic model of foreland-basin sequences: Geology, v. 16, p. 510–505.
Izett, G. A., 1981, Volcanic ash beds: Recorders of upper Cenozoic silicic pyroclastic volcanism in the western United States: Journal of Geophysical Research, v. 86, p. 10200–10222.
Johnson, N. M., Opdyke, N. D., and Lindsay, E. H., 1975, Magnetic polarity stratigraphy of Pliocene-Pleistocene terrestrial deposits and vertebrate faunas, San Pedro Valley, Arizona: Geological Society of America Bulletin, v. 86, p. 5–12.
Johnson, S. Y., 1985, Eocene strike-slip faulting and non-marine basin formation in Washington, *in* Biddle, K. T., and Christie-Blick, N., eds., Strike-slip deformation, basin formation, and sedimentation: Society of Economic Paleontologists and Mineralogists Special Publication 37, p. 283–302.
Jordan, T. E., Flemings, P. B., and Beer, J. A., 1988, Dating thrust-fault activity by use of foreland-basin strata, *in* Kleinspehn, K. L., and Paola, C., eds., New perspectives in basin analysis: Heidelberg, Federal Republic of Germany, Springer-Verlag, p. 307–330.
Kraus, M. J., and Middleton, L. T., 1987, Contrasting architecture of two alluvial suites in different structural settings, *in* Ethridge, F. G., Flores, R. M., and Harvey, M. D., eds., Recent developments in fluvial sedimentology: Society of Economic Paleontologists and Mineralogists Special Publication 39, p. 253–262.
Langbein, W. B., and Schumm, S. A., 1958, Yield of sediment in relation to mean annual precipitation: Eos (American Geophysical Union Transactions), v. 39, p. 1076–1084.
Lindsay, E. H., 1978, Late Cenozoic vertebrate faunas, southeastern Arizona: New Mexico Geological Society 29th Guidebook, p. 269–276.
Lindsay, E. H., 1984, Windows to the past: Fossils of the San Pedro Valley: Arizona Geological Survey Fieldnotes, v. 14, no. 4, p. 1–9.
Lindsay, E. H., Smith, G. A., and Haynes, C. V., Jr., 1990a, Late Cenozoic depositional history deposits and geoarcheology, San Pedro Valley, Arizona, *in* Gehrels, G., and Spencer, J. E., eds., Geological excursions through the Sonoran Desert region, Arizona and Sonora: Arizona Geological Survey Special Paper 7, p. 9–19.
Lindsay, E. H., Smith, G. A., Haynes, C. V., and Opdyke, N. D., 1990b, Sediments, geomorphology, magnetostratigraphy, and vertebrate paleontology in the San Pedro Valley, Arizona: Journal of Geology, v. 98, p. 605–619.
Lysonski, J. C., Aiken, C. L. V., and Sumner, J. S., 1981, The complete Bouguer gravity anomaly map of Arizona: Arizona Geological Survey Open-File Report 81-24, 22 maps, scale 1:250,000.
Machette, M. N., 1985, Calcic soils of the southwestern United States, *in* Weide, D. L., ed., Soils and Quaternary geology of the southwestern United States: Geological Society of America Special Paper 203, p. 1–21.
Mack, G. H., and Rasmussen, K. A., 1984, Alluvial-fan sedimentation of the Cutler Formation (Pennsylvanian) near Gateway, Colorado: Geological Society of America Bulletin, v. 95, p. 109–116.
Magaritz, M., Kaufman, A., and Yaalon, D. H., 1981, Calcium carbonate nodules in soils: $^{18}O/^{16}O$ and $^{13}C/^{12}C$ ratios and ^{14}C contents: Geoderma, v. 25, p. 157–172.
Mann, A. W., and Horowitz, R. C., 1979, Groundwater calcrete deposits in Australia: Some observations from Western Australia: Geological Society of Australia Journal, v. 26, p. 292–303.
Mayer, L., Gerson, R., and Bull, W. B., 1984, Alluvial gravel production and deposition: A useful indicator of Quaternary climatic changes in deserts: Catena, suppl. 5, p. 137–151.
Melton, M. A., 1965, The geomorphic and paleoclimatic significance of alluvial deposits in southern Arizona: Journal of Geology, v. 73, p. 1–38.
Menges, C. M., 1983, The neotectonic framework of Arizona: Implications for the regional character of Basin-Range tectonism: Arizona Geological Survey Open-File Report 83-19, 109 p.
Menges, C. M., and McFadden, L. D., 1981, Evidence for a latest Miocene to Pliocene transition from Basin-Range tectonic to post-tectonic landscape evolution in southeastern Arizona: Arizona Geological Society Digest, v. 13, p. 151–160.
Morrison, R. B., 1985, Pliocene/Quaternary geology, geomorphology, and tectonics of Arizona, *in* Weide, D. L., ed., Soils and Quaternary geology of the southwestern United States: Geological Society of America Special Paper 203, p. 123–146.
Motts, W. S., 1970, Some hydrologic and geologic processes influencing playa development in western United States, *in* Reeves, C. C., Jr., ed., Playa lake symposium: Lubbock, Texas, International Center for Arid and Semi-Arid Land Studies Publication 4, p. 89–106.
Neal, J. T., 1970, Playa surface features as indicators of environment, *in* Reeves, C. C., Jr., ed., Playa lake symposium: Lubbock, Texas, International Center for Arid and Semi-Arid Land Studies Publication 4, p. 107–132.
Paola, C., 1988, Subsidence and gravel transport in alluvial basins, *in* Kleinspehn, K. L., and Paola, C., eds., New perspectives in basin analysis: Heidelberg, Federal Republic of Germany, Springer-Verlag, p. 231–244.
Paola, C., Heller, P. L., and Angevine, C. L., 1992, The large-scale dynamics of grain-size variation in alluvial basins, 1: Theory: Basin Research, v. 4, p. 73–90.
Peirce, H. W., 1984, Some late Cenozoic basins and basin deposits of southern and western Arizona, *in* Smiley, T. L., and others, eds., Landscapes of Arizona: Tucson, Arizona, University Press of America, p. 207–227.
Perlmutter, M. A., and Matthews, M. D., 1990, Global cyclostratigraphy—A model, *in* Cross, T. A., ed., Quantitative dynamic stratigraphy: Englewood Cliffs, New Jersey, Prentice Hall, p. 233–260.
Quade, J., 1986, Late Quaternary environmental changes in the upper Las Vegas Valley, Nevada: Quaternary Research, v. 26, p. 340–357.
Quade, J., Cerling, T. E., and Bowman, J. R., 1989, Systematic variations in the carbon and oxygen isotopic composition of pedogenic carbonate along elevation transects in the southern Great Basin, United States: Geological Society of America Bulletin, v. 101, p. 464–475.
Retallack, G. J., 1990, Soils of the past: Boston, Massachusetts, Unwin Hyman, 520 p.
Sadler, P. M., 1981, Sediment accumulation rates and the completeness of stratigraphic sections: Journal of Geology, v. 89, p. 569–584.
Sadler, P. M., and Strauss, D. J., 1990, Estimation of completeness of stratigraphic sections using empirical data and theoretical models: Geological Society of London Journal, v. 147, p. 471–485.
Scarborough, R. B., 1984, Cenozoic erosion and sedimentation in Arizona: Arizona Geological Survey Open-File Report 85-3, 61 p.
Scarborough, R. B., Menges, C. M., and Pearthree, P. A., 1983, Map of Basin and Range (post 15 m.y.a.) exposed faults, grabens, and basalt-dominated volcanism in Arizona: Arizona Geological Survey Open-File Report 83-21, scale 1:500,000.
Semeniuk, V., and Meagher, T. D., 1981, Calcrete in Quaternary coastal dunes in southwestern Australia: A capillary-rise phenomenon associated with plants: Journal of Sedimentary Petrology, v. 51, p. 47–68.
Semeniuk, V., and Searle, D. J., 1985, Distribution of calcrete in Holocene coastal sands in relationship to climate, southwestern Australia: Journal of Sedimentary Petrology, v. 55, p. 86–95.
Slate, J. L., and Smith, G. A., 1992, Use of carbonate morphology and clay content to determine paleosol genesis in the Plio-Pleistocene St. David Formation, southeastern Arizona: Geological Society of America Abstracts with Programs, v. 24, p. A285–A286.
Smith, G. A., Deacon, M. W., and Lindsay, E. H., 1988, Nontectonic influences on deposition of continental basin fill: An example from southeastern Arizona: Geological Society of America Abstracts with Programs, v. 20, p. 316.
Smith, G. A., Wang, Y., and Cerling, T. E., 1992, Implications of the sedimentology and isotope geochemistry of calcic horizons in the Pliocene–early Pleistocene St. David Fm., Arizona: Geological Society of America Abstracts with Programs, v. 24, p. A286.
Smith, G. A., Wang, Y., Cerling, T. E., and Geissman, J. W., 1994, Comparison of a paleosol-carbonate isotope record to other records of Pliocene–early Pleistocene climate in the western United States: Geology, v. 22 (in press).
Steel, R. J., Maehle, S., Nilsen, H., Roe, S. L., and Spinnangr, A., 1977, Coarsening-upward cycles in the alluvium of Hornelen Basin (Devonian) Norway: Sedimentary response to tectonic events: Geological Society of America Bulletin, v. 88, p. 1124–1134.
Tuan, Y.-F., 1962, Structure, climate, and basin land forms in Arizona and New Mexico: Association of American Geographers Annals, v. 52, p. 51–68.
Wang, Y., Cerling, T. E., Smith, G. A., Quade, J., and Lindsay, E. H., 1993, Stable isotopes of paleosol carbonates and fossil teeth as paleoecology and paleoclimate indicators: An example from the upper Cenozoic nonmarine sediments in the San Pedro Valley, Arizona, *in* Swart, P., Lohman, K. C., and Mackenzie, J. A., eds., Climate change in continental isotopic records: American Geophysical Union Monograph 78, p. 241–248.
Wells, S. G., McFadden, L. D., and Dohrenwend, J. C., 1987, Influence of late Quaternary climatic changes on geomorphic and pedogenic processes on a desert piedmont, eastern Mojave Desert, California: Quaternary Research, v. 27, p. 130–146.
Wilson, L., 1973, Variations in mean annual sediment yield as a function of mean annual precipitation: American Journal of Science, v. 273, p. 335–349.
Wiltschko, D. V., and Dorr, J. A., Jr., 1983, Timing of deformation in overthrust belt and foreland of Idaho, Wyoming, and Utah: American Association of Petroleum Geologists Bulletin, v. 67, p. 1304–1322.
Wright, V. P., and Tucker, M. E., 1991, Calcretes: An introduction, *in* Wright, V. P., and Tucker, M. E., eds., Calcretes: International Association of Sedimentologists Reprint Series, v. 2, p. 1–22.
Yair, A., and Enzel, Y., 1987, The relationship between annual rainfall and sediment yield in arid and semi-arid areas. The case of the northern Negev, *in* Ahnert, F., ed., Geomorphological models—Theoretical and empirical aspects: Catena, suppl. 10, p. 121–135.

Manuscript Received by the Society June 7, 1993
Revised Manuscript Received December 6, 1993
Manuscript Accepted December 20, 1993

Printed in U.S.A.